Metal–insulator transition in thin films of R_xR_{1-x} 'NiO_3 compounds: DC electrical conductivity and IR spectroscopy measurements

2005 J. Phys.: Condens. Matter 17 1137

(http://iopscience.iop.org/0953-8984/17/7/007)

INSTITUTE OF PHYSICS PUBLISHING JOURNAL OF PHYSICS: CONDENSED MATTER

J. Phys.: Condens. Matter **17** (2005) 1137–1150 doi:10.1088/0953-8984/17/7/007

Metal–insulator transition in thin films of $R_xR'_{1-x}NiO_3$ compounds: DC electrical conductivity and IR spectroscopy measurements

F Capon[1], P Ruello[1,5], J-F Bardeau[1], P Simon[2], P Laffez[1], B Dkhil[3], L Reversat[1], K Galicka[1,4] and A Ratuszna[4]

[1] Laboratoire de Physique de l'Etat Condensé, UMR 6087 CNRS/Université du Maine LPEC-72085 Le Mans, France
[2] Centre de Recherches sur les Matériaux à Haute Température (CRMHT) CNRS, 45071 Orléans Cedex 2, France
[3] Laboratoire Structure, Propriétés et Modélisation des Solides, UMR 8580 CNRS/Ecole Centrale Paris, Gde Voie des Vignes 92295 Châtenay-Malabry, France
[4] Institute of Physics (A Chelkowski), Solid State Physics Department, University of Silesia, Poland

E-mail: pascal.ruello@univ-lemans.fr

Received 9 June 2004, in final form 13 January 2005
Published 4 February 2005
Online at stacks.iop.org/JPhysCM/17/1137

Abstract

In this work a systematic comparison of DC electrical conductivity and IR optical properties of thin films of ($R_xR'_{1-x}NiO_3$), where R′ = Nd and R = Sm or Eu, is performed. Independently of the nature of R, it is confirmed that the metal–insulator transition temperature (T_{MI}) in $R_xR'_{1-x}NiO_3$ as well as in $RNiO_3$ is driven by the mean lattice distortion quantified by the tolerance factor of the perovskite. The internal chemical pressure decrease due to substitution of Nd by another rare earth element with smaller cationic radius gives rise to an increasing resistivity in the metallic state together with a decrease of the screening effect in the IR reflectance. We suggest this is due to a modification of the free electron properties at the Fermi level and of the Fermi surface properties consistent with photoemission literature data. On the other hand, similar transmittance spectra for various systems are reported in the insulating state. A systematic temperature independent drop of the transmittance above 0.6 eV is found for each system whatever the value of T_{MI}.

1. Introduction

Due to its metal–insulator transition and thermochromic properties, the rare earth nickelate perovskite $RNiO_3$ has received a great deal of attention for the last ten years [1]. Such

[5] Author to whom any correspondence should be addressed.

unusual electronic and optical features are all the more interesting since the metal–insulator transition temperature (T_{MI}) can be tuned by changing the R cation: $LaNiO_3$ is metallic while $PrNiO_3$, $NdNiO_3$, $SmNiO_3$ and $EuNiO_3$ undergo an MI transition at 130, 200, 400 and 460 K respectively [2]. Solid solutions of various rare earth nickelates allow also the control of the metal insulator temperature [3–5]. It has been shown that the MIT is closely related to the structure distortion and in particular to the arrangement of NiO_6 octahedra. This distortion modifies the super-exchange angle Ni–O–Ni and the Ni–O bond length which drive the overlapping of the O(2p) and Ni(3d) band and therefore control the closing and opening of the charge transfer gap [6]. In the $RNiO_3$ family, when the R cation radius decreases, the MIT is not only shifted towards higher values but it appears systematically that the resistivity also increases over the whole temperature range [2]. In the $Sm_xNd_{1-x}NiO_3$ [4] and $Eu_xLa_{1-x}NiO_3$ [7] systems, when the rare earth radius decreases, T_{MI} increases consistently with the decrease of the Goldschmidt factor, and there is also an overall shift of the resistivity towards higher values over the whole temperature range. This is probably due to a shift of free carriers properties (concentration, Fermi velocity) (for the metallic state at least) connected to a change of the O(2p)/Ni(3d) band overlapping driven by various perovskite distortions. No minimum of the metallic conductivity of $Sm_xNd_{1-x}NiO_3$ at $x \sim 0.5$, as observed by Gire *et al* [8] (entropic effect), was reported by Ambrosini and Hamet [4]. It has been suggested that changing the rare earth cation acts as internal chemical pressure (increasing internal pressure by substituting the rare earth cation with another one of larger ionic radius) which can lead, as for the isostatic pressure experiment [9], to a tunability of the metal–insulator transition temperature [10, 11]. Obradors *et al* [9] reported on a decrease of T_{MI} upon increasing isostatic pressure but with remaining metallic properties of $PrNiO_3$ and $NdNiO_3$ (same magnitude and thermal dependence of the electrical resistivity). Canfield *et al* [10] observed the same phenomena with only a slight decrease of the metallic resistivity upon elevating external pressure. The effect of the external pressure was directly correlated to the variation of the tolerance factor: an increasing pressure increases the tolerance factor and decreases T_{MI}. But, as pointed out by Medarde *et al* [11], the analogy is not simple since controversial conclusions are proposed by Canfield *et al* and Obradors *et al* who respectively found a negative [10] and positive [9] value for the pressure dependence of the tilt angle w ($\partial w/\partial P_{ext}$). A more recent structural investigation of Medarde *et al* [11] has revealed clear difference between internal and external pressure and in particular underlined that in the internal pressure mechanism the angle tilting is the most affected parameter compared to the variation of the Ni–O bond length. To probe and better understand the electrical and optical properties upon varying the chemical composition and the internal chemical pressure, we have performed our study on various solid solution compounds. We have classified our solid solutions according to their degree of departure from the perfect cubic perovskite (tolerance factor). This tolerance factor was the only parameter.

2. Experiment

Two chemical systems ($Sm_xNd_{1-x}NiO_3$ and $Eu_xNd_{1-x}NiO_3$) with compositions corresponding to three different tolerance factors for each have been synthesized. For each tolerance factor, the rare earth ratio (Nd/Sm and Nd/Eu) was chosen in order to give comparable distortions assuming, as a first hypothesis, that a mixing rule could be applied for structural distortion. The distortion from the cubic cell was estimated using the Goldschmidt tolerance factor for oxides [12]. In this approach, considering the ABO_3 perovskite, a cubic cell is observed when $d_{A-O} = d_{B-O}\sqrt{2}$. This is the case for example for $SrTiO_3$ where the ionic radii of Sr and Ti match perfectly to give a regular array of octahedrons. When

Table 1. T_{MI} was determined either when the slope of ρ changes its sign—T_{MI}(ii) at $d(\rho)/dT = 0$—or at the inflexion point of the resistivity—T_{MI} (i); h and c mean in the heating and in the cooling regime. Column 5 corresponds to the width of the hysteresis loop—T_{MI}(i)h − T_{MI}(i)c. The mixing rule $T_{MI} = xT_{MI}(RNiO_3) + (1-x)T_{MI}(R'NiO_3)$ was assumed to calculate T_{MI}. Q is the metallic quality factor (see the text).

t	Composition	$T_{MI(i)c}/T_{MI(i)h}$ elect. cond. (K)	$T_{MI(ii)}$ elect. cond. (K)	$T_{MI(i)h}-T_{MI(i)c}$ elect. cond. (K)	T_{MI} calculation: see the text (K)	T_{MI} IR transmission minimum (K)	E_g (eV) ±0.02 eV	T_0 (K)	Q (K^{-1}) at 330 K ($\times 10^{-3}$)
0.9711	$NdNiO_3$	156/196	210	40					3.5 [27]
0.9697	$Sm_{0.2}Nd_{0.8}NiO_3$	197/207	250	10	240	250	0.078	7.07×10^6	2.24 ± 0.3
	$Eu_{0.15}Nd_{0.85}NiO_3$	202/211	254	9	247	245	0.07	7.78×10^6	0.78 ± 0.3
0.9684	$Sm_{0.37}Nd_{0.63}NiO_3$	255/262	307	7	280	300	0.074	2.04×10^7	1.29 ± 0.2
	$Eu_{0.3}Nd_{0.7}NiO_3$	264/268	320	4	285	300	0.054	1.43×10^4	0.97 ± 0.2
0.9677	$Sm_{0.5}Nd_{0.5}NiO_3$	285	343	0	305	325	0.054	3.87×10^5	1.98 ± 0.3
	$Eu_{0.38}Nd_{0.62}NiO_3$	277	343	0	305	325	0.05	9.8×10^4	0.51 ± 0.3

$d_{A-O} \neq d_{B-O}\sqrt{2}$ the distortion is quantified by the tolerance factor $t = \frac{d_{R-O}}{d_{Ni-O}\sqrt{2}}$ (for cubic structure $t = 1$). Values of $t = 0.9711$, 0.9642, and 0.9620 respectively were calculated for $NdNiO_3$, $SmNiO_3$, and $EuNiO_3$ using data from [13–15] for the Ni–O and R–O length. The mixing rule for the determination of the tolerance factor for the solid solutions is for example $t(Sm_{0.2}Nd_{0.8}NiO_3) = (0.2t(SmNiO_3) + 0.8t(NdNiO_3))$. Compositions and tolerance factors are shown in table 1. We have chosen compositions which correspond to systems exhibiting the same transition temperature for the metal–insulator transition and for the antiferromagnetic ordering ($T_{MI} \sim T_N$). This allows us to exclude the magnetic ordering as an additional parameter.

Thin films were grown by sputtering from an oxide ceramic target onto the single-crystal substrate of undoped Si{100} with both sides polished. The substrate temperature was fixed at 600 °C, the deposition time at 30 min and the film thickness at approximately 150 nm. The films were annealed for 2 days at 820 °C under an oxygen pressure of 210 bar (see [3] for more details). Laffez *et al* showed [16] that the annealing conditions—800 °C and 2 days—after sputtering are enough to produce a textured perovkite phase $NdNiO_3$ and the film shows only a minor NiO phase (x-ray diffraction). TEM measurements confirm the results of the x-ray diffraction and show well crystallized domains. Therefore the synthesis conditions are not necessarily as drastic as for the bulk. The used temperature and pressure represent an upper limit, above which we observe the growth of a SiO_2 interlayer between the substrate and the film. This interlayer, which takes it origin in the oxidation of the Si substrate, could generate impurities or desegregate the film, and forms the critical step of the process. The chemical stoichiometry of the deposited material was checked by energy dispersive x-ray analysis (EDX) using a LINK EDX spectrometer coupled with a SEM microscope. Details of the experimental conditions can be found in [17]. X-ray diffraction was performed before and after annealing, using Cu Kα in an X-Pert Philips diffractometer. The pseudo-cubic out-of-plane lattice parameter of the solid solutions ($Sm_{0.5}Nd_{0.5}NiO_3$, $Eu_{0.3}Nd_{0.7}NiO_3$) was determined directly by studying the thermal displacement of the (004) Bragg peak. The DC electrical resistance was measured with the four-probe method scanning temperature from 20 to 380 K using Quantum Design equipment. Cooling and heating regimes were studied. IR spectra were recorded by a Bruker IFS 66 spectrometer with DTGS detector in the frequency range 400–7000 cm^{-1} (1.42–25 μm). Only the heating regime was studied.

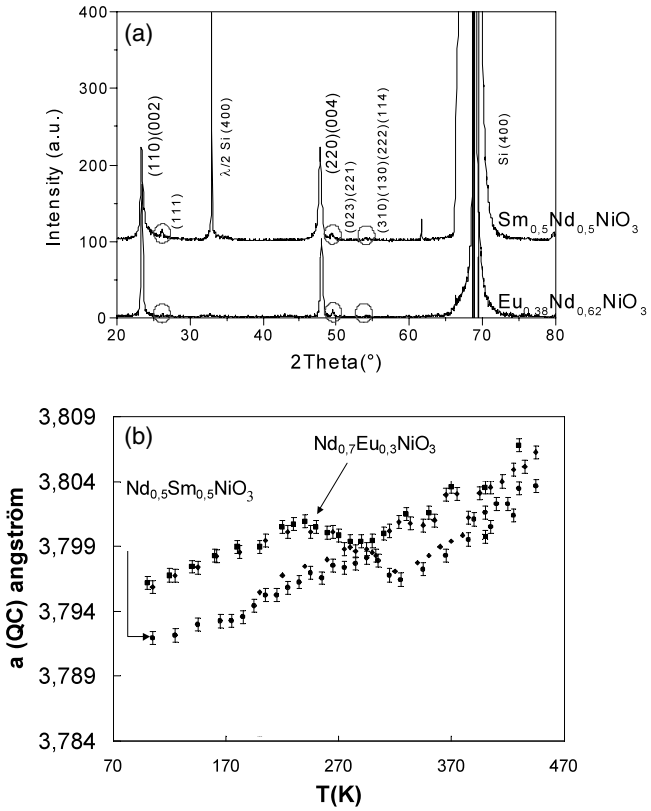

Figure 1. (a) Room temperature x-ray diffraction pattern for $Nd_{0.62}Eu_{0.38}NiO_3$ and $Nd_{0.5}Sm_{0.5}NiO_3$ ($t = 0.9677$) thin films. Indexation refers to an orthorhombic cell P_{bnm} with average $a = \sqrt{2}a_p$, $b = \sqrt{2}a_p$, and $c = 2a_p$. The average pseudocubic parameter a_p is 3.79 Å for all $R_xR'_{1-x}NiO_3$ compounds. (b) Thermal variation of the pseudo-cubic out-of-plane parameter of $Nd_{0.5}Sm_{0.5}NiO_3$ and $Nd_{0.7}Eu_{0.3}NiO_3$ determined by the (004) Bragg peak position.

3. Results

3.1. X-ray diffraction

The x-ray diffraction patterns of the perovskite films with a small tolerance factor are shown in figure 1(a). In each film the structure was found to be consistent with a perovskite cell and reveals a strong orientation along the pseudo-cubic [100] axis of the perovskite subcell as previously reported for $NdNiO_3$. The $R_xR'_{1-x}NiO_3$ compounds are well crystallized although we observe a decrease of the peak intensity and the appearance of additional peaks due to disorientation when t decreases. X-ray diffraction experiments versus temperature have confirmed the structural change at T_{MI}, (figure 1(b)). The evolution of the average unit cell volume was found to be consistent with the evolution of the composition.

3.2. Resistivity versus temperature

The electrical resistivity displayed in figure 2(a) is characteristic for rare earth nickelates [1–6]. T_{MI} was determined either at inflexion point of the resistivity—T_{MI}(i) or when the slope of ρ changes its sign—T_{MI}(ii) at $d(\rho)/dT = 0$; h and c mean in the heating and in the cooling

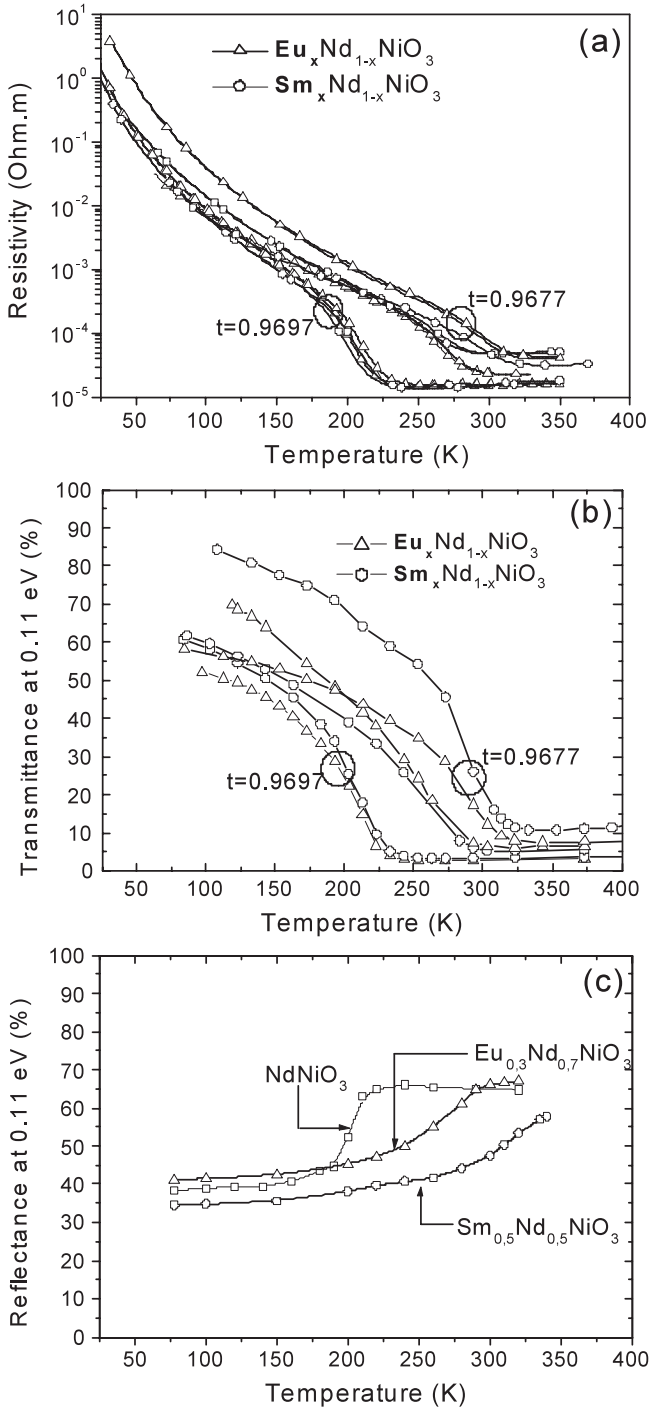

Figure 2. (a) Electrical resistivity, (b) IR transmission and (c) reflection at 0.11 eV respectively. For each figure, the diamond refers to $Nd_{1-x}Eu_xNiO_3$ and $Nd_{1-x}Sm_xNiO_3$ solid solutions. The systems exhibiting same tolerance factor are indicated by the black circle.

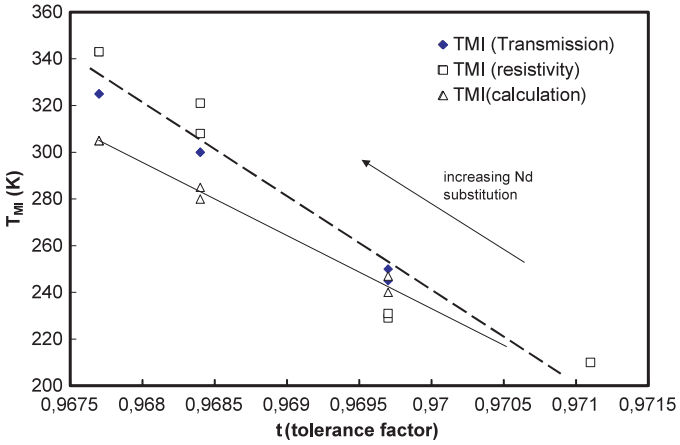

Figure 3. Thermal variation of the metal–insulator transition determined from figure 2(a). For IR transmission T_{MI} is determined at the minimum value of transmission. For the electrical conductivity it corresponds to $(\mathrm{d}(\rho)/\mathrm{d}T)_{T=T_{MI}} = 0$.

(This figure is in colour only in the electronic version)

regime. T_{MI} increases linearly when the tolerance factor decreases (figure 3). The experimental value of $T_{MI(ii)}$ is in good agreement with the value of T_{MI} calculated by a linear mixing rule: $T_{MI(ii)} = xT_{MI(ii)}(RNiO_3) + (1-x)T_{MI(ii)}(R'NiO_3)$ (table 1 and figure 3), even if a departure from this empirical law is observed when the distortion increases. This is a good demonstration that the T_{MI} depends less on the chemical nature of the solid solution than on the mean distortion factor t of the perovskite. The steric effect drives the MIT of these solid solutions as already seen on pure $RNiO_3$ compounds [6]. The size distribution of the NiO_6 octahedra induced by changing the structural disorder for various solid solutions seems to be of negligible importance compared to the mean distortion. As already reported in the literature [4, 18], with increasing distortion the MIT is less abrupt and the width of the hysteresis loop decreases (table 1). Moreover, in agreement with the results for $Sm_xNd_{1-x}NiO_3$, and $Eu_xLa_{1-x}NiO_3$ [7, 5] and pure $RNiO_3$ compounds [2], an increase of the electrical resistance of the metallic state over the whole temperature range (20–380 K) is evidenced when t decreases, although the film with the composition $Sm_{0.37}Nd_{0.63}NiO_3$ exhibits a deviation from this behaviour (this could be due to the presence of minor traces of impurities which are found in sample; see figure 1 in reference [3]). Finally, in the insulating state, only a slight increase of the resistivity was observed when the tolerance factor decreased.

3.3. Infrared optical properties

Figure 4 shows the infrared (IR) reflectance in the range (0–0.9 eV). The screening effect which corresponds to the increase of density of charge carriers in the low energy spectrum (i.e. the well known spectral weight transfer in the IR range during MIT [19]) is well evidenced. The reflectance IR spectra exhibit several peaks which are either associated with SiO_2 or IR active modes of the perovskite. A large SiO_2 band appears at 135 meV.[6] For small energy, the film presents two absorption bands dominated by the antisymmetric T_{1u} stretching ν(Ni–O) and deformation δ(Ni–O) modes of the perovskite NiO_6 octahedra [20–22]. In agreement

[6] A simulated spectrum of a thin film (∼150 nm) deposited on SiO_2 substrate shows an inversion of the SiO_2 band—135 meV. This behaviour is due to interference between the film and the SiO_2 interface.

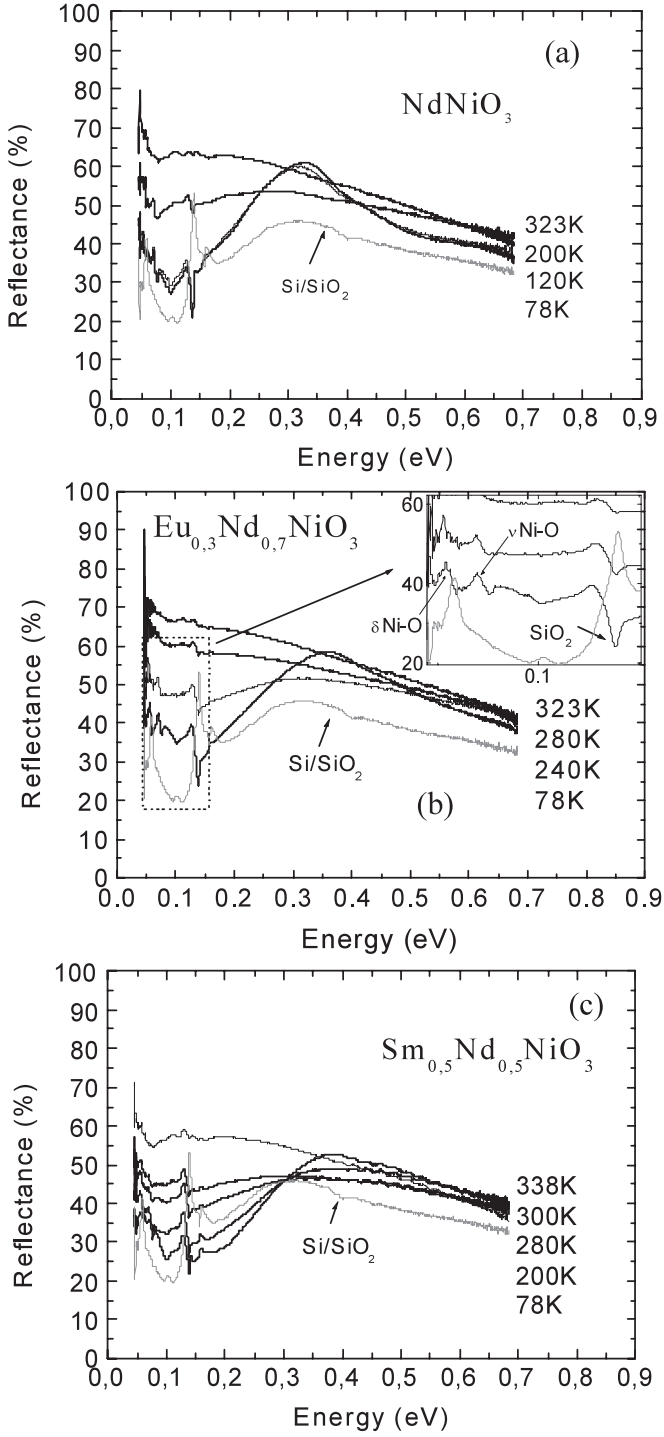

Figure 4. Thermal variation of the IR reflectance: (a) $NdNiO_3$, (b) $Nd_{0.7}Eu_{0.3}NiO_3$, (c) $Nd_{0.5}Sm_{0.5}NiO_3$. The inset of (b) shows the low energy spectrum with peaks of the interlayer SiO_2 and IR active vibration modes of the perovskite.

with previous studies, the temperature dependence of reflectance only appears in the energy range of 0/∼0.4 eV [19]. The cut-off value of about 0.4 eV is independent of the transition temperature. This change of the IR reflectance is also accompanied by a drastic variation of the IR transmittance as displayed in figure 5. Absorption bands at 76, 92, 100 and 135 meV are attributed to the SiO_2 interlayer [17] (interface film/substrate and non-deposited surface; see the inset in figure 5). For higher wavelengths the film presents two absorption bands attributed, as well as in reflectance spectra, to the IR active modes ν(Ni–O)—69 meV—and δ(Ni–O)—56 meV. For our compositions $RR'NiO_3$ (i.e. whatever the transition temperature) the temperature sensitive IR transmission is observed only below 0.6 eV which strongly suggests that no thermochromic properties above 0.6 eV can occur. It is important to note that the shapes of the transmission spectra for the insulating state are very similar whatever the sample, even if the MIT occurs at different temperature. Because of the Si and SiO_2 contributions to the IR transmittance and reflectance, any suitable phonon studies were not carried out, nor absorption determination as shown in the literature [23–25]. Nevertheless, the thermal variation of transmittance and reflectance was measured separately at 0.11 eV where IR active phonon absorption of the thin film and absorption by the native SiO_2 inter-layer ($NdNiO_3/SiO_2/Si$) are negligible. The drop of these optical transmittance and reflectance (measured at 0.11 eV, figures 2(b) and (c)) occurs at increasing temperature as the tolerance factor decreases, consistently with the MIT detected by the electrical conductivity experiments. The temperature at the minimum value of the transmission is compared with that of electrical conductivity (figure 3).

4. Discussion

4.1. Metallic state

The analysis of the electrical resistance and optical properties reveal that with increasing distortion the electrical resistivity in the metallic state becomes higher. Several parameters can be involved for the increase of resistivity: (i) a decrease in the number of free carriers when the distortion increases; (ii) an electron scattering magnitude increase upon increasing distortion; (iii) a change of the Fermi velocity; (iv) a change of the Fermi surface topology. A variation of the effective mass could also be evocated. In order to compare, at least, the scattering mechanisms in each sample, the quality factor of the metallic state has been determined. The quantum model of conduction in a single band has been adopted [26] where we consider the DC electrical conductivity driven by the mean scattering rate at Fermi level (we consider a $\vec{k}$-independent scattering time as a first approximation) and by the properties of the Fermi surface as follows (equation (1)).

$$\sigma_0 = e^2\overline{\tau(E_F)}\int \frac{d\vec{k}_F}{4\pi^3}\frac{V^2(\vec{k}_F)}{3}\delta(E-E_F) \tag{1}$$

where σ_0, $V(\vec{k}_F)$, $\overline{\tau(E_F)}$ and $\delta(E-E_F)$ are the DC electrical conductivity, the Fermi velocity, the mean scattering time at Fermi level and the Dirac function. This relation leads to the Drude-like relation for a spherical shape of the Fermi surface.[7] Two kinds of scattering mechanisms, one due to the thermal phonons of the lattice ($\frac{1}{\tau_L} \approx \frac{kT}{\Gamma}$) and the second due to the defects

[7] If we consider the Fermi surface as a sphere with an isotropic Fermi velocity, equation (1) leads to the Drude-like formula $\sigma_0 = e^2\overline{\tau(E_F)}\int_{SF}\frac{d\vec{k}_F}{4\pi^3}\frac{V^2(\vec{k}_F)}{3}\delta(E-E_F) = e^2\frac{\overline{\tau(E_F)}}{m^*}\frac{k_F^3}{3\pi^2} = \frac{e^2\overline{\tau(E_F)}N_e}{m^*}$, where $N_e = 2\times\frac{\frac{4}{3}\pi k_F^3}{8\pi^3}$ and $V_F = \frac{\hbar k_F}{m^*}$, with N_e, $\overline{\tau(E_F)}$ and m^* the volumic concentration of the total free electrons within the Fermi sphere, the mean scattering time between two collisions of carriers at Fermi level and the effective mass of carriers, respectively.

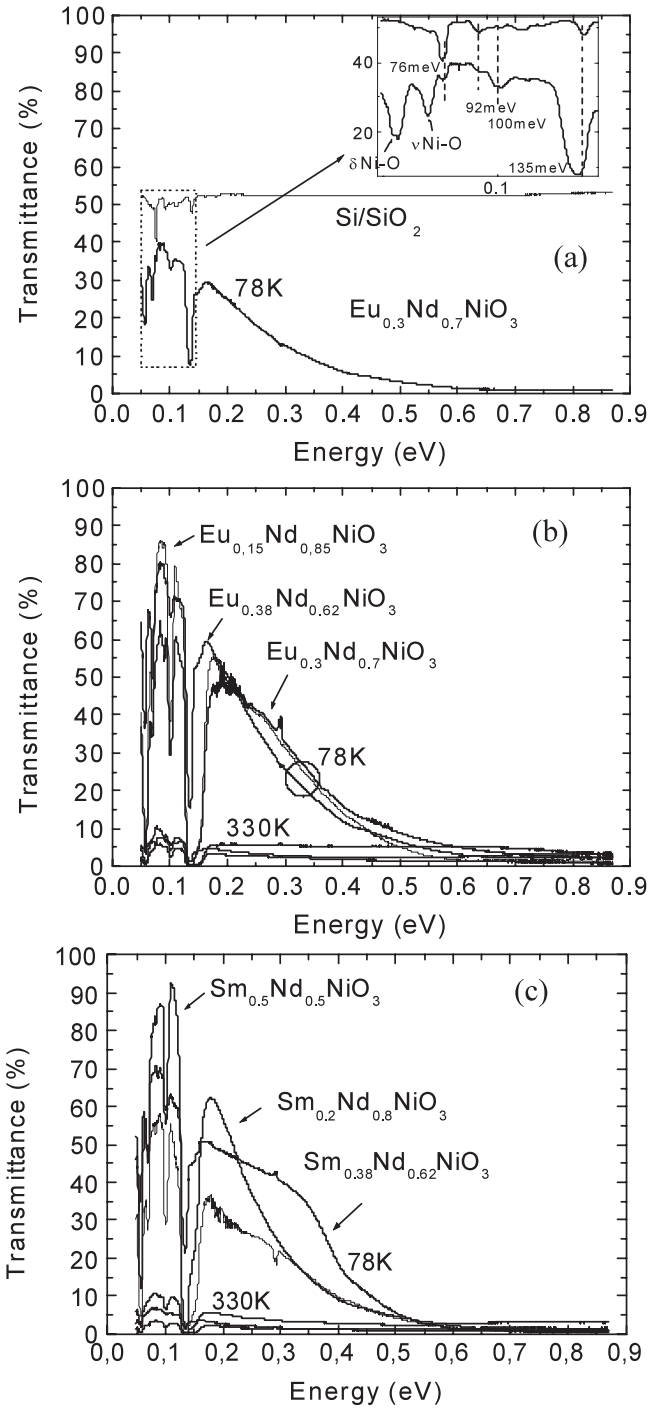

Figure 5. Thermal variation of the IR transmittance: (a) spectrum of $Nd_{0.7}Eu_{0.3}NiO_3$ and that of the interlayer and the substrate Si/SiO_2 (the inset shows the low energy spectrum with peaks of the interlayer SiO_2 and IR active vibration modes of the perovskite); ((b), (c)) comparison between the transmittance spectra of the system $Nd_{1-x}Eu_xNiO_3$ ($Nd_{1-x}Sm_xNiO_3$) at room and liquid nitrogen temperature.

τ_d, are considered. According to the Matthiessen rule (we consider here that the two kinds of scattering phenomena are non-interacting), the total scattering time is then

$$\frac{1}{\overline{\overline{\tau\,(E_F)}}} \simeq \frac{1}{\tau_d} + \frac{1}{\tau_L}. \tag{2}$$

Then, the quality factor becomes

$$Q = \frac{1}{\rho_0}\frac{d\rho_0}{dT} = \frac{k}{\frac{\Gamma}{\tau_d} + kT}. \tag{3}$$

That quality factor depends only on the ratio of the mean scattering characteristic times. For each system, that Q-factor is displayed in table 1. The value of the Q-factor of $NdNiO_3$ bulk given by Catalan *et al* [27] is also provided in the table. It appears that Q factors are a bit smaller than the $NdNiO_3$ bulk one. Within each system ($Nd_{1-x}Sm_xNiO_3$ or $Nd_{1-x}Eu_xNiO_3$) no large variation is observed when changing the tolerance factor. Within a given system, this means that the ratio of the scattering times does not change too much when the tolerance factor changes, in the range investigated at least. Then if we consider that the unchanged value $\frac{\Gamma}{\tau_d}$ is due to unchanged τ_L and τ_d, this means that the increase of the resistivity is then essentially driven by a decrease of the Fermi velocity and/or the Fermi surface. As a consequence, the change of the tolerance factor might have an influence on the electronic band structure at Fermi level and the dynamics at Fermi level, contrary to the effect of the high isostatic external pressure as reported in the experiments of Obradors *et al* [9]. It also has to be mentioned that quality factor of the solid solution $Nd_{1-x}Eu_xNiO_3$ is always smaller than that of $Nd_{1-x}Sm_xNiO_3$. It is not easy to explain that difference and to precisely know which of the scattering mechanisms is more important in the samarium system compared to the europium system because we have only the ratio between the thermal phonon scattering and the defect scattering.

Furthermore, the screening effect observed above the MIT (figures 2(c) and 4) in the low energy spectrum due to nearly free carriers appears to be in qualitative agreement with the Hagen–Rubens relation approach (figure 2(c)):

$$R(\omega) = 1 - 2\sqrt{\frac{2\omega\varepsilon_0}{\sigma_0}} \tag{4}$$

where $R(\omega)$ is the spectral reflectance at normal angle incidence as a function of the frequency ω. The change of the electrical resistivity when t varies is indeed directly correlated to the change of the reflectivity.

Then, it provides new information about the effect of internal pressure, as discussed in the literature [9–11, 28]. While isostatic external pressure conserves the metallic properties, we observe that by tuning the internal chemical pressure T_{MI} not only decreases with increasing tolerance factor but the Fermi surface and the dynamics at E_F might change: an increase of the Fermi surface and the Fermi velocity could occur. For an increase of the T_{MI} of 100 K, the metallic resistivity is divided by $\sim$2.5. This result is in agreement with recent photoemission studies where a slight increase of the number of electrons at Fermi level was evidenced when x decreases in the solid solution compound $Sm_xNd_{1-x}NiO_3$ [29]. Nevertheless, above the MIT, the ratio between the number of electrons per volume at the Fermi level of the compounds $x = 0$ and 0.4 is close to 1.15 while we have a ratio of $\sim$2.5 for the conductivity for $x = 0.2$ and 0.5 respectively.

4.2. Insulating state

In the low temperature region the thermal variation of transmittance shows a slight increase for more distorted structures except for the compound $Sm_{0.5}Nd_{0.5}NiO_3$. For the

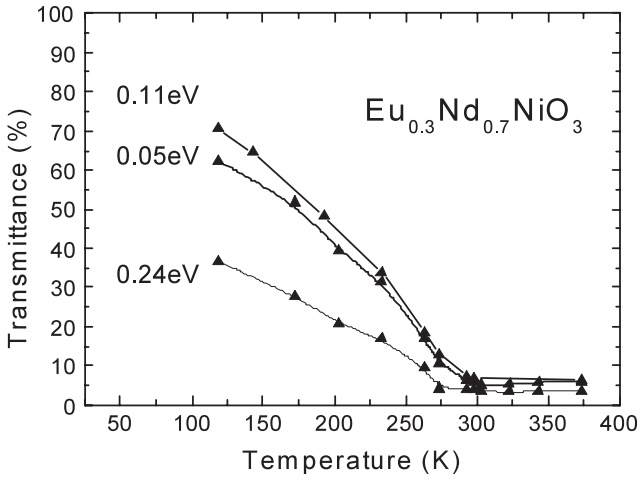

Figure 6. Energy dependence of the drop of the transmittance.

reflectance, smaller differences are reported compared to the high temperature regime (see figure 4). The variation of transmittance originates from differences in the electronic band structure of the insulating state. From the DC electrical conductivity measurements, we can get some information about these electronic band structures. In the case of the nickelate family, the electronic transport properties have been described considering two simultaneous contributions, namely the classical activated regime and the variable range hopping (VRH) [27, 30, 31]. The first regime is commonly used to describe the electrical properties of semiconductors (Si, Ge). The VRH is applied for amorphous semiconductors (Si, Ge, Se–Si) [32] where localized states in the intra-gap region offer a new method of charge transport. In that case, electronic drift is determined by phonon-induced tunnelling of electrons between localized states in the intra-gap region near the Fermi level (figure 8). VRH electrical transport is the main contribution at low temperature. Using equation (5) suggested by Catalan *et al* [27] we have fitted the electrical conductivity. The semiconducting state is modelled as the direct sum of two terms, one arising from VRH and another from normal activated conduction with a constant activation energy E_a:

$$1/R = A\exp(-E_a/T) + B\exp(-(T_0/T)^{1/4}) \tag{5}$$

where A, E_a, B and T_0 are fitted parameters.

In the fitting procedure, we have checked that the VRH contribution did contribute mainly to the electrical conductivity at low temperature. Independently of the chemical composition, E_a shows only a slight variation—between 0.05 and 0.07 eV (table 1). According to the classical conduction theory of semi-conductor conduction, and neglecting the migration activation energy in E_a, this would lead to a gap of $E_g = 2E_a \sim 0.1$–0.14 eV. These values are in agreement with those found in the literature [1, 3, 19, 30]. The T_0 values are displayed in table 1. Large differences appear between these VRH temperatures. These VRH temperatures are also large compared to that of Blasco *et al* [30] but of the same order as that of amorphous and disordered semiconductors [32] where such high values are interpreted as a consequence of extrinsic contribution to the total electrical conductivity. We cannot exclude extrinsic contribution in our materials, but at the moment no chemical analysis of our samples has been done to support doping by impurities.

Following the idea of internal chemical pressure (decrease of the Ni–O–Ni superexchange angle upon increasing the structural distortion), a decrease of the gap should be expected with increasing tolerance factor, which is not clearly observed here. That absence of clear

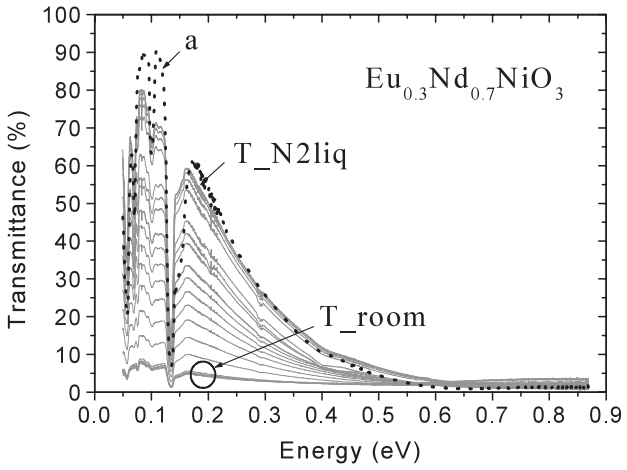

Figure 7. Thermal variation of the transmission spectrum of $Eu_{0.3}Nd_{0.7}NiO_3$. The temperature increases from the top (78 K: T_{N2liq} = liquid nitrogen temperature) to the bottom (298 K = $T_{room\ temperature}$). The dotted curve (a) represents the IR spectra of $NdNiO_3$ at liquid nitrogen temperature.

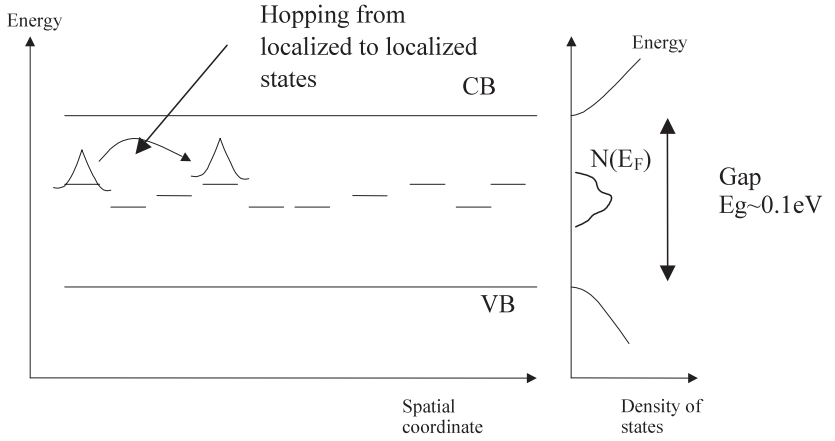

Figure 8. Sketch of the electronic band structure in the insulating state including the gap and the intra-gap states (VRH model).

distinguishable gap of 0.1–0.14 eV is also confirmed by the transmittance experiments. A continuous decrease of the transmittance indeed occurs from ∼0.05 to 0.6 eV (figures 5, 6 and 7). This diffuse absorption tail is probably not connected to structural disorder induced by the fluctuation of the NiO_6 octahedron size, because a similar spectrum is observed for the pure $NdNiO_3$ compound. The broad absorption tail could be due to the existence of several mechanisms of absorption in the energy range 0 to ∼0.6 eV, probably including the contribution of localized states in the intra-gap region which might spread over a quite large energy range in the intra-gap region giving rise to a gradual absorption edge from 0 to ∼0.6 eV. This gradual absorption is consistent with a broad absorption edge tail like that observed for $NdNiO_3$ bulk in optical conductivity studies by Katsufuji *et al* [19]. There is indeed a similarity between the optical conductivity tail in the range 0–0.6 eV and the one found in the IR transmittance experiment. Furthermore, above ∼0.6 eV, it seems that the IR transmittance of the solid solutions is nearly independent of the temperature (figure 5). This feature is consistent with Okazaki *et al* [29], Vobornik *et al* [33] and Okazaki *et al* [34] who have shown, by photoemission experiments, that the density of states located beyond 0.6/0.7 eV below

the Fermi level does not change with varying temperature while the density of states included between 0 and ∼0.6 eV exhibits variation above and below the transition temperature. The present IR spectroscopy strongly supports the assumption that the electronic states involved in the MIT are those included in the range 0–0.6 eV. But, in contrast to Okazaki *et al* [28, 33] and Vobornik *et al* [32], we did not observe a spectral weight transfer from the range 0.7–0.3 towards 0.3–0 eV with increasing temperature. Nevertheless, the similar transmission spectra for different compositions in the low energy region (specially for the family $Nd_{1-x}Eu_xNiO_3$), despite the different T_{MI}, are the most important characteristic of the $RR'NiO_3$ thin films. This indicates that the electronic band structures of the different compositions (i.e. different structural distortion and then different Ni–O–Ni angle and Ni–O bond length) are very similar, consistent with the observations of Okazaki *et al* [34] in the systems $Nd_{1-x}Eu_xNiO_3$ with $x \leqslant 0.4$. This later observation leads us to suggest that it is not easy to connect the knowledge of the low-energy electronic band structure at low temperature with the value of the metal–insulator transition temperature because they are nearly the same for several systems. Nor is it easily correlated to the gap as suggested in the literature [1] by the relation $E_g \propto kT_{MI}$. It is certain that the spectral weight transfer towards the low energy region does not trigger at the same temperature when changing the mean distortion. It looks as if the change of the internal pressure does not affect the electronic band structure but only the triggering temperature at which the transfer of electrons towards the Fermi level occurs. If the electronic structure is nearly the same, one possibility to explain such different triggering is to consider the electron–phonon interaction as the driving mechanism as already described in the literature [35, 36]. In order to conclude on this phenomenon, further investigations are required. A systematic study of the thermal dependence of the IR active modes is in progress to describe more precisely the possible difference of phonon dynamics in solid solutions exhibiting the same mean perovskite distortion (same tolerance factor).

5. Summary

In this work, six different thin films of the family $R_xR'_{1-x}NiO_3$ have been synthesized with three different structural departures from the cubic perovskite structure quantified by the Goldschmidt factor t. For each value of t, two solid solutions were prepared. Electrical measurements show that the metal–insulator transition temperature is in agreement with the value calculated by the simple mixing rule $T_{MI} = xT_{MI}(RNiO_3) + (1 - x)T_{MI}(R'NiO_3)$ and reveal that the nature of the rare earth metal is of negligible importance for our systems. For our composition $RR'NiO_3$, a thermochromic effect has been observed in the low energy spectrum (<0.6 eV). It has been found that the screening effect of the metallic state decreases when the distortion increases. This is consistent with a decrease of the electrical conductivity. The analysis of the electrical resistivity and the quality factor of the metallic state indicates that there is a change of the Fermi surface properties (V_F, number of free electrons per volume): the Fermi velocity (V_F) as well as the value of the Fermi surface could increase for the less distorted system. Moreover, no large difference between electron scattering times seems to appear for the various solid solutions. In the low temperature regime, a systematic temperature independent IR absorption is observed for all systems and independently of their T_{MI} above 0.6 eV. Similar spectra are found in the range 0–0.6 eV. This common feature supports the idea that the electronic structure does not vary too much between these systems, in this range of energy at least, but the triggering of the spectral weight transfer towards low energy region is on the other hand very different. It may be connected to an increase of the electron–phonon interaction with decreasing internal chemical pressure. This point must be further clarified with new experiments and phonon dynamics studies.

Acknowledgments

This work was supported by l'Agence pour le Developpement et la Maîtrise de l'Energie (ADEME) and the area Pays de la Loire.

The authors thank Dr F Poncin Epaillard for providing access to IR spectroscopy equipment and Dr Ph Lacorre for providing the high pressure–temperature furnace as well as G Niesseron for his help during film synthesis.

References

[1] Medarde M L 1997 *J. Phys.: Condens. Matter* **9** 1707
[2] Lacorre P, Torrance J B, Pannetier J, Nazzal A J, Wang P W and Huang T C 1991 *J. Solid State Chem.* **91** 225
[3] Capon F, Laffez P, Bardeau J F, Simon P, Lacorre P and Zaghrioui M 2002 *Appl. Phys. Lett.* **81** 619
[4] Ambrosini A and Hamet J F 2003 *Appl. Phys. Lett.* **82** 727
[5] Capon F 2003 *PhD Thesis* University of Maine, France
[6] Torrance J B, Lacorre P, Nazzal A I, Ansaldo E J and Niedermayer Ch 1992 *Phys. Rev.* B **45** 8209
[7] Sánchez R D, Causa M T, Seoane A, Rivas J, Rivadulla F, López-Quintela M A, Pérez Cacho J J, Blasco J and Garcia J 2000 *J. Solid State Chem.* **151** 1
[8] Gire A, Jouffroy M, Théobald J G, Bohnke O, Frand G and Lacorre P 1997 *J. Phys. Chem. Solids* **58** 577
[9] Obradors X, Paulius L M, Maple M B, Torrance J B, Nazzal A I, Fontcuberta J and Granados X 1993 *Phys. Rev.* B **47** 12353
[10] Canfield P C, Thompson J D, Cheong S-W and Rupp L W 1993 *Phys. Rev.* B **47** 12357
[11] Medarde M, Mesot J, Lacorre P, Rosenkranz S, Fischer P and Gobrecht K 1995 *Phys. Rev.* B **52** 9248
[12] Goldschmidt V M 1926 *Skr. Nor. Vidensk. Akad. Oslo* **2** 11926
[13] Garcia-Munoz J L, Rodriguez-Carvajal J, Lacorre P and Torrance P J B 1992 *Phys. Rev.* B **46** 4414
[14] Rodríguez-Carvajal J, Rosenkranz S, Medarde M, Lacorre P, Fernandez-Díaz T, Fauth F and Trounov V 1998 *Phys. Rev.* B **57** 456
[15] Demazeau G, Marbeuf A, Pouchard M and Hagenmuller P 1971 *J. Solid State Chem.* **3** 582
[16] Laffez P, Zaghrioui M, Retoux R and Lacorre P 2000 *J. Magn. Magn. Mater.* **211** 111
[17] Laffez P, Retoux R, Boullay P, Zaghrioui M, Lacorre P and Vantendeloo G 2000 *Eur. Phys. J. Appl. Phys.* **12** 55
[18] Frand G, Bohnke O, Lacorre P, Fourquet J L, Carré A, Eid B, Théobald J G and Gire A 1995 *J. Solid State Chem.* **120** 157
[19] Katsufuji T, Okimoto Y, Arima T and Tokura Y 1995 *Phys. Rev.* B **51** 4830
[20] Baran E J 1990 *Catal. Today* **8** 133
[21] Last J T 1957 *Phys. Rev.* **105** 1740
[22] Ross S D 1972 *Inorganic Infrared and Raman Spectra* (London: McGraw-Hill)
[23] Massa N E, Alonso J A, Martinez-Lope M J and Rasines I 1997 *Phys. Rev.* B **56** 986
[24] Mroginski M A, Massa N E, Salva H, Alonso J A and Martinez-Lope M J 1999 *Phys. Rev.* B **60** 5304
[25] De la Cruz F P, Piamonteze C, Massa N E, Salva H, Alonso J A, Martinez-Lope M J and Casais M T 2002 *Phys. Rev.* B **66** 153104
[26] Ashcroft N W and Mermin D 1976 *Solid State Physics* (Philadelphia, PA: Saunders) ISBN 0-03-083993-9
[27] Catalan G, Bowman R M and Cregg J M 2000 *Phys. Rev.* B **62** 7892
[28] Mortimer R, Weller M T and Henry P 1999 *Physica* B **271** 173
[29] Okazaki K, Mizokawa T, Fujimori A, Sampathkumaran E V and Alonso J A 2002 *J. Phys. Chem. Solids* **63** 975
[30] Blasco J, Castro M and Garcia J 1994 *J. Phys.: Condens. Matter* **6** 5875
[31] Mallick R, Sampathkumaran E V, Alonso J A and Martinez-Lope M J 1998 *J. Phys.: Condens. Matter* **10** 3969
[32] Paul D K and Mitra S S 1973 *Phys. Rev. Lett.* **31** 1000
[33] Vobornik I, Perfetti L, Zacchigna M, Grioni M, Margaritondo G, Mesot J, Medarde M and Lacorre P 1999 *Phys. Rev.* B **60** R8426
[34] Okazaki K, Mizokawa T, Fujimori A, Sampathkumaran E V, Martinez-Lope M J and Alonso J A 2003 *Phys. Rev.* B **67** 1
[35] Medarde M, Lacorre P, Conder K, Fauth F and Furrer A 1998 *Phys. Rev. Lett.* **80** 2397
[36] Medarde M, Lacorre P, Conder K, Rodriguez-Carvajal J, Rosenkranz S, Fauth F and Furrer A 1998 *Physica* B **241–243** 751